Journal of Hazardous Materials 198 (2011) 95–102

Contents lists available at SciVerse ScienceDirect

Journal of Hazardous Materials

journal homepage: www.elsevier.com/locate/jhazmat

Hazardous dichloromethane recovery in combined temperature and vacuum pressure swing adsorption process

Shivaji G. Ramalingam[a,*], Jerôme Saussac[d], Pascaline Pré[a], Sylvain Giraudet[b,c], Laurence Le Coq[a], Pierre Le Cloirec[b,c], Serge Nicolas[e], Olivier Baudouin[d], Stéphane Déchelotte[d], Alice Medevielle[e]

[a] Ecole des Mines de Nantes, GEPEA, UMR-CNRS 6144, 4 rue Alfred Kastler, BP 20722, 44307 Nantes Cedex 03, France
[b] Ecole Nationale Supérieure de Chimie de Rennes, CNRS, UMR 6226, Avenue du General Leclerc, CS 50837 35708 Rennes Cedex 7, France
[c] Université Européenne de Bretagne, France
[d] PROSIM, Stratège Bâtiment A, BP 27210, F-31672 Labege Cedex, France
[e] ARKEMA, GRL Groupement de Recherches de Lacq, BP 34 64170 Lacq, France

ARTICLE INFO

Article history:
Received 15 July 2011
Received in revised form 3 October 2011
Accepted 3 October 2011
Available online 8 October 2011

Keywords:
Adsorption
Breakthrough curve
Simulation
Fixed bed
Hot nitrogen
Vacuum regeneration

ABSTRACT

Organic vapors emitted from solvents used in chemical and pharmaceutical processes, or from hydrocarbon fuel storage stations at oil terminals, can be efficiently captured by adsorption onto activated carbon beds. To recover vapors after the adsorption step, two modes of regeneration were selected and could be possibly combined: thermal desorption by hot nitrogen flow and vacuum depressurization (VTSA). Because of ignition risks, the conditions in which the beds operate during the adsorption and regeneration steps need to be strictly controlled, as well as optimized to maintain good performances. In this work, the optimal conditions to be applied during the desorption step were determined from factorial experimental design (FED), and validated from the process simulation results. The regeneration performances were compared in terms of bed regeneration rate, concentration of recovered volatile organic compounds (VOC) and operating costs. As an example, this methodology was applied in case of dichloromethane. It has been shown that the combination of thermal and vacuum regeneration allows reaching 82% recovery of dichloromethane. Moreover, the vacuum desorption ended up in cooling the activated carbon bed from 93 °C to 63 °C and so that it significantly reduces the cooling time before starting a new cycle.

1. Introduction

Industrial emissions of volatile organic compounds (VOC) of different types from gas, oil, paint, solvent and other chemical sectors [1–3] cause serious health and environmental risks. Especially, dichloromethane has adverse toxic effects on human central nervous system and environment; the European parliament thus decided to ban its use with concentration equal to or greater than 0.1% weight [4]. This research work focuses on the removal of dichloromethane by adsorption and the regeneration of fixed beds. Studies based on the effect of the operating conditions of VOC adsorption have already been carried out [5–8].

Carbon adsorption is a phenomenon that adsorbs contaminants on the surface of granular activated carbon [9–11]. After adsorption, to recover the VOC molecules (contaminants) at higher concentration, a kinetic energy is required in the form of temperature (thermal energy) or vacuum for regeneration. Regeneration is defined as the process followed by adsorption to remove the organic vapors from the adsorbent either by raising the temperature or decreasing pressure or other driving force such as vacuum [12]. In general, regeneration is of two steps: desorption and activation [13].

Activation is a required step particularly in the case of steam regeneration, because there is a possibility of condensed water in the bed; then the condensed water can be removed by passing the hot dry air through the bed. The activation step could be neglected in the case of absence of moisture in the bed. The factors influencing the effectiveness of regeneration are: (1) the degree of purification, (2) the adsorbent stability, (3) the degree of recovery of adsorbed components and (4) energy consumption [14,15].

There are different modes of thermal regeneration such as steam regeneration or hot nitrogen regeneration. Using steam regeneration, there is serious concern in the activated carbon bed after regeneration step [13]. Therefore, the drying step is essential to remove any moisture present in the carbon bed. As a result drying step increases the regeneration time. But the main advantages of steam regeneration are its availability in industrial unit and low production cost [13]. The advantages of using hot nitrogen are: it is inert; it causes no moisture formation in the bed and so there is no need of drying step [13].

* Corresponding author. Tel.: +33 633923537.
E-mail address: shivaji.ramalingam@yahoo.co.in (S.G. Ramalingam).

0304-3894/$ – see front matter © 2011 Elsevier B.V. All rights reserved.
doi:10.1016/j.jhazmat.2011.10.019

Nomenclature

a_p	ratio between the external surface and the volume of the particle (m^{-1})
bo	parameter of the model (atm^{-1})
b_1	parameter of the model (T^{-1})
Cp_a	specific heat capacity of adsorbed phase ($J\,kg^{-1}\,K^{-1}$)
Cp_p	specific heat capacity of the adsorbent ($J\,kg^{-1}\,K^{-1}$)
C_i	VOC concentration in the gas phase ($mol\,m^{-3}$)
Cp_g	specific heat capacity of gas phase ($J\,kg^{-1}\,K^{-1}$)
D_L	axial mass dispersion coefficient ($m^2\,s^{-1}$)
D_{gl}	global mass transfer coefficient ($m^2\,s^{-1}$)
d_c	diameter of the column (m)
D_L	diffusivity ($m^2\,s^{-1}$)
D_H	axial heat dispersion coefficient ($J\,m^{-1}\,s^{-1}$)
d_p	equivalent particle diameter (m)
e	thickness of the column (m)
H	enthalpy of gas phase ($J\,kg^{-1}$)
h_w	heat transfer coefficient of wall ($W\,m^2\,K^{-1}$)
h_p	heat transfer coefficient with solid particle ($W\,m^2\,K^{-1}$)
ΔH_i	enthalpy of adsorption/desorption of the compound i ($J\,mol^{-1}$)
ΔH_{vap}	latent heat of vaporisation ($kJ\,mol^{-1}$)
K_f	external mass transfer coefficient ($m\,s^{-1}$)
K	global mass transfer coefficient (s^{-1})
PI	VOC ionisation potential (eV)
P_i	equilibrium VOC partial pressure (atm)
q_i	adsorbed VOC concentration ($mol\,kg^{-1}$)
qi^*	adsorbed VOC concentration at the equilibrium with the gas phase ($mol\,kg^{-1}$)
q_i^*	VOC adsorbed quantity at the equilibrium ($mol\,kg^{-1}$)
q_{mo}	parameter of the model ($mol\,kg^{-1}$)
q_{m1}	parameter of the model (T^{-1})
q_i	VOC concentration in the adsorbed phase ($mol\,kg^{-1}$)
r_p	partcicle equivalent radius (m)
r_{mic}	adsorbent average micropore opening (nm)
T	temperature of gas (°C)
T_p	temperature of solid particle (°C)
v	superficial velocity ($m\,s^{-1}$)
V_m	molar VOC volume ($m^3\,mol^{-1}$)
v	superficial gas velocity ($m\,s^{-1}$)
y	VOC molar fraction in the gas
ρ_p	bulk adsorbent density ($kg\,m^{-3}$)
ρ_g	density of gas phase ($kg\,m^{-3}$)
ε	bed porosity
λ	thermal conductivity of the material of the column (W/m/K)
α	VOC polarisability ($10^{-24}\,cm^3$)
γ	surface tension of the liquid solvent ($mN\,m^{-1}$)
μ	kinematic viscosity (Pa s)

The use of vacuum regeneration followed by thermal regeneration is more relevant than vice versa in terms of achieving final regeneration percentage [16]. A factorial experimental design was made by changing three operating conditions of the thermal regeneration step and followed by the vacuum regeneration step at constant operating conditions. During the vacuum regeneration, a small flow rate of nitrogen at $0.018\,N\,L\,s^{-1}$ and a pressure of 0.04 bars are used [16].

FED is a statistical analysis which helps to study the influence of the operating conditions on the desired responses to be measured. Fig. 1 shows the different combination of two different operating conditions (X_1, X_2) in an experiment and the signs (− and +) corresponds to minimum and maximum of the operating conditions [17]. The final response is measured as '*Y*'. By using FED method in MINITAB, the analysis of variance (ANOVA) can be performed to obtain a response equation (Y) which is in linear form with the function of operating conditions (X_1, X_2).

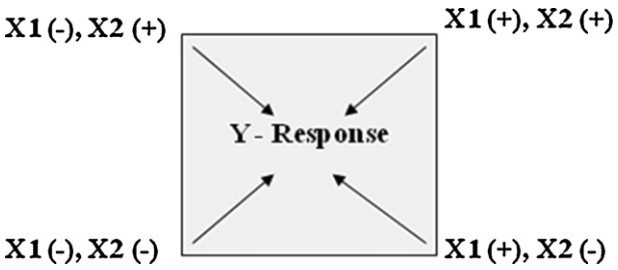

Fig. 1. FED representation.

$$Y = a_0 + a_1 \cdot X_1 + a_2 \cdot X_2 + a_3 \cdot X_1 \cdot X_2 \quad (1)$$

where Y – measured response; X_1, X_2 – operating conditions and a_0, a_1, a_2, a_3 – constants

The experiments and the methodologies which details: (1) the properties of activated carbon; (2) adsorption isotherm data for VOC – activated carbon system (AC), and also the simulations model consists of mass and energy balances are presented in the following sections. FED will be used to study the effect of nitrogen temperature (T); flow rate of nitrogen (V_f); and intermediate regeneration (I_R) on the responses such as recovery percent (F_R) and the operating costs ($OP_€$). The three operating conditions which change during thermal regeneration step are: (1) nitrogen temperature, (2) flow rate of nitrogen; and (3) intermediate regeneration percentage (I_R). Intermediate regeneration percentage (I_R) is defined as the percentage for which vacuum regeneration is applied just after hot nitrogen regeneration to achieve maximum recovery efficiency at optimized cost. Intermediate regeneration was chosen as 55% (−) and 75% (+) for analyzing the vacuum regeneration effect. The objectives of the combined regeneration are: (1) to study the influence of operating conditions on the recovery efficiency and operating costs by using FED; (2) to find the time for which vacuum regeneration can be applied to achieve maximum recovery efficiency, to reduce the operating costs, and also to achieve the cooling benefits of the activated carbon bed after hot nitrogen regeneration. The aim of the study is to develop the simulation tool for adsorption and regeneration of VOC–AC system based on all the experimental work and the simulation model.

2. Theoretical

2.1. Characterization of activated carbon

The activated carbon CECA – ACM 404 is a coal based physically activated carbon. The physical properties of the activated carbon (CECA – ACM404) such as B.E.T. surface specific area, micro pore volume (by Horvath–Kawazoe method), micropore average width (by Density Functional Theory) were measured by nitrogen adsorption isotherm at 77 K (Micromeritics ASAP 2010) [18,19]; the mesopore and macropore volume, and bulk density were measured by using mercury porosimeter (Micromeritics Autopore IV 9500) [20]. Finally the ratio of oxygen to carbon was measured using elemental analyzer (Thermofinnigan Flash EA1112 CHNS-O Analyzer) [21].

The properties resumed in Table 1 are used in simulation models of adsorption and regeneration.

Table 1
Characteristics of the activated carbon ACM404.

Activated carbon	Size of micro pore (nm)	Bulk density (mg L^{-1})	Micro pore volume (cm^3 g^{-1})	BET surface area (m^2 g^{-1})	Total volume (cm^3 g^{-1})	Ratio O:H %
ACM 404	0.66	0.423	0.44	1063	0.55	0.7

2.2. Properties of dichloromethane

ACROS organics supplied 99% pure dichloromethane for the experiments and following are the properties of dichloromethane (CH_2Cl_2) in Table 2.

2.3. Simulation model

The cyclic adsorption–desorption process is simulated by solving the mass and energy balances during each step: adsorption, possibly bed preheating by the walls, thermal desorption by steam or nitrogen flow, and/or desorption under vacuum. The main equations and assumptions used are described below.

2.3.1. Mass balance

$$-D_L\frac{\partial^2 C_i}{\partial z^2}+\frac{\partial(vC_i)}{\partial z}+\frac{\partial C_i}{\partial t}+\frac{1-\varepsilon}{\varepsilon}\rho_p\frac{\partial q_i}{\partial t}=0 \quad (2)$$

2.3.2. Linear driving force model (LDF)

The adsorption or desorption kinetics is described according to the linear driving force model [22]:

$$\frac{\partial q_i}{\partial t}=K\cdot(q_i^*-q_i) \quad (3)$$

The overall resistance to the mass transfer between the gas and the solid phases embodies the partial resistance to the mass transfer at the external surface of the particles and the internal mass transfer resistance, expressed as a function of an effective diffusion coefficient D_{gl}:

$$\frac{1}{K}=\frac{\rho_p V_m q_i^*}{K_f a_p y}+\frac{r_p}{5D_{gl}a_p} \quad (4)$$

The external mass transfer coefficient K_f was derived from the correlation from Petrovic and Thodos [18]. The effective diffusion coefficient takes into account the various diffusion mechanisms which control the migration of the organic component to the adsorption sites (porous, Knudsen, and surface diffusion). It is considered as an adjustable parameter. As a first approximation, effective the mass transfer resistance data was considered to be unchanged in the desorption step.

2.3.3. Equilibrium model

The value q_i^* in the linear driving force model (LDF) is computed from the modified Langmuir isotherm model, taking into account the temperature effect on the equilibrium data. The parameters of the Langmuir equation were derived from the experimental data measured for the system (dichloromethane – ACM 404) at 20, 40, 60 and 80 °C. The R-Stat statistical software was used to check the significance of the computed parameters using an interval of confidence of 95% by Student t-test. The results are summarized in Table 3.

$$q_i^*=\frac{q_{mo}\exp\left(\frac{q_{m1}}{T}\right)k_0\exp\left(\frac{k_1}{T}\right)P_i}{1+k_0\exp\left(\frac{k_1}{T}\right)P_i} \quad (5)$$

2.3.4. Enthalpy balances

- *In the gas phase*:

$$-\rho_g D_L\frac{\partial^2 H}{\partial z^2}+\varepsilon\rho_g\frac{\partial H}{\partial t}+\varepsilon\frac{\partial(v\rho_g H)}{\partial z}+\frac{4}{d_c}\left[\frac{1}{h_p}+\frac{d_c\cdot e}{(d_c+e)\cdot\lambda}\right]^{-1}\times(T-T_w)+(1-\varepsilon)\frac{6h_p}{d_p}(T-T_p)=0 \quad (6)$$

- *In the solid phase*:

$$(\rho_p Cp_p+\rho_p Cp_a q_i)\frac{\partial T_p}{\partial t}+\frac{6h_p}{d_p}(T_p-T)+\Delta H_i\rho_p\frac{\partial q_i}{\partial t}=0 \quad (7)$$

The adsorption enthalpy was derived according to the following statistical predictive model [8]:

$$-\Delta H_{ads}=103.2+1.16\alpha+0.76\Delta H_{vap}-3.87PI-0.7\gamma-26.19r_{mic} \quad (8)$$

As a first approximation, the integral enthalpy of desorption was assumed to be equal to the one computed for the adsorption.

2.3.5. Ergun's pressure drop equation

$$\frac{\partial P}{\partial z}+150\times10^{-5}\left(\frac{1-\varepsilon}{\varepsilon}\right)^2\frac{\mu}{d_p^2}v+1.75\times10^{-5}\left(\frac{1-\varepsilon}{\varepsilon}\right)\frac{\rho_g}{d_p}v^2=0 \quad (9)$$

The effect of pressure drop on the dynamic behavior of the adsorption and regeneration steps has been considered in the simulation model by Ergun's equation [22].

3. Experimental

Fig. 2 shows the experimental setup of ACM404 (activated carbon) – dichloromethane (VOC) system. The adsorption column used is made of stainless steel and the dimensions are 1.5 m in length, 0.05 m of internal diameter and 0.015 m thickness. The thermal conductivity value (λ) was taken from the database which had been implemented in the simulation package. The first step was the adsorption of dichloromethane on ACM404, and then followed by regeneration step which is a combination of hot N_2 and vacuum. In the system, a continuous gas-phase sampling of VOC concentration using FID was present in Fig. 2. FID was used to measure the

Table 2
Properties of dichloromethane.

Form	Stable colorless liquid
Density	1326.6 kg m^{-3}
Molecular weight	84.93 g mol^{-1}
Melting point	−97 °C
Boiling point	40 °C

Table 3
Langmuir isotherm coefficients.

Langmuir model coefficients – dichoromethane – ACM404 system			
q_{m0} (mol kg^{-1})	q_{m1} (T^{-1})	k_1 (T^{-1})	k_0 (atm^{-1})
2.695	239.21	2723.24	0.01441

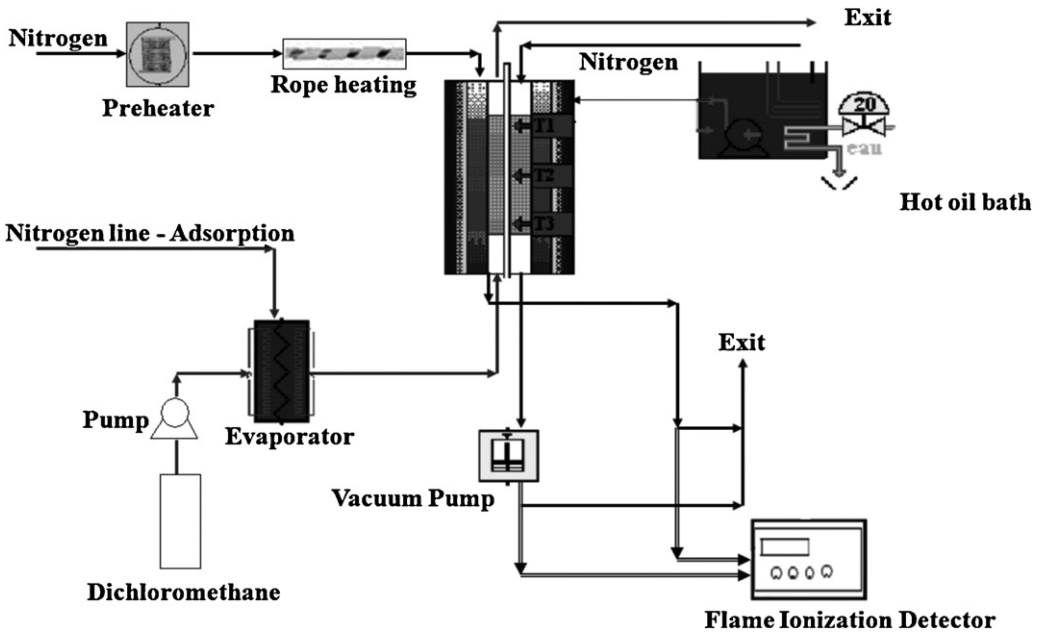

Fig. 2. Pilot plant scheme.

exit concentration of dichloromethane from the column and it was calibrated before the adsorption experiments. A system of heating cable was arranged around the pipeline to heat the nitrogen externally before entering the column. It was done to avoid the heat loss of hot nitrogen with atmosphere before entering the column for regeneration.

3.1. Adsorption step

The adsorption step of dichloromethane on ACM 404 was achieved with the operating conditions as mentioned in Table 4. A constant flow rate of 0.0257 g $^{-1}$ of dichloromethane was passed through the evaporator which is at 35 °C. A small flow rate of nitrogen (0.05 N L s^{-1}) was passed through the evaporator to carry the dichloromethane which is in vapor form. The small flow rate of nitrogen was purged with another nitrogen stream of 0.56 N L s^{-1}, thus forming a concentration of 50 g m^{-3} of dichloromethane in the gas stream (dichloromethane + nitrogen) which is entering the column for adsorption. The gas which is at 0.56 N L s^{-1} was sent from the bottom of the column which was packed with 1.222 kg of ACM404 (activated carbon) as shown in Fig. 2.

The thermocouples T_1, T_2 and T_3 were placed at the top (T_1 = 5 cm), middle (T_2 = 105 cm), and bottom (T_3 = 145 cm) of the column, respectively. As the thickness of steel column is very large (1.5 cm) and so there was not significant heat transfer by the hot nitrogen to the activated carbon bed during the regeneration step. So the column was heated along by hot oil bath at 80 °C for 40 min. The nitrogen for regeneration from the pre-heater was then passed on to rope heating to avoid heat loss before entering the column.

Table 4
Pilot specifications and adsorption step operating conditions.

Adsorption column size	1.5 m × 0.05 m
Adsorption gas velocity	0.28 m s^{-1}
Concentration CH_2Cl_2	50 g m^{-3}
Pump flow rate CH_2Cl_2	0.0257 g s^{-1}
Total gas flow rate (N_2 + CH_2Cl_2)	0.56 L s^{-1}

3.2. Regeneration step

After the adsorption step, the regeneration was performed with the combination of thermal (hot N_2) and vacuum regeneration. There were six regeneration experiments had been designed by changing the operating conditions such as temperature of hot nitrogen [85 °C and 93 °C], flow rates of nitrogen [0.07 N L s^{-1} and 0.14 N L s^{-1}], and intermediate regeneration percentages [55% and 75%]. During the second step of regeneration which was the vacuum regeneration, the operating conditions had been fixed at 0.04 bars by passing 0.018 N L s^{-1} of nitrogen at room temperature. The total regeneration time was fixed in all the six cases as 180 min, which includes 40 min of the hot oil bath along the column. All these operating conditions were summarized in Table 5.

3.3. Factorial Experimental Design (FED)

FED has been implemented to study the effects of set of factors on the responses; (1) to estimate the magnitude of the effects contributed by the factors; (2) and to develop a mechanistic model [11]. In Table 5, X_1 and X_2 are two different factors and the response (output) was measured as Y. The FED analysis was performed by with MINITAB software by using analysis of variance (ANOVA) method.

At the end of the ANOVA, it gives a model in the form of the following equation:

$$F_R = a_0 + a_1 \cdot T + a_2 \cdot I_R + a_3 \cdot T \cdot I_R \quad (10)$$

$$OP_€ = b_0 + b_1 \cdot T + b_2 \cdot V_f + b_3 \cdot T \cdot V_f \quad (11)$$

where F_R – recovery efficiency; $OP_€$ – operating costs; T – temperature of nitrogen factor; I_R – intermediate regeneration factor and V_f – volumetric flow rate of nitrogen factor.

3.4. Estimation of recovery efficiency and operating costs

The recovery efficiency was estimated from the integration of the regenerated mass (g) with time (min). The operating costs for the regeneration step was calculated by the summation of energy costs of all the heating equipments (pre-heater, rope heating, hot oil bath, and vacuum pump) and the consumption of nitrogen during

Table 5
Regeneration – operating conditions.

Exp.	Step 1: thermal regeneration (hot N_2)				Step 2: vacuum regeneration	
	T_{N_2} (°C)	Flow N_2 (N L h^{-1})	Time (min)	I_R (%), step1	Flow N_2 (N L s^{-1})	Time (min)
1	93	0.14	100	75	0.018	40
2	85	0.14	105	75	0.018	35
3	93	0.14	50	55	0.018	90
4	85	0.14	55	55	0.018	85
5	93	0.07	108	55	0.018	72
6	85	0.07	121	55	0.018	59

Table 6
Inputs for operating costs estimation.

Power of vacuum pump (kW)	0.396
Power of hot oil bath (kW)	2
Power of pre-heater (kW)	0.3
Power of rope heating (kW)	0.2
Cost of Nitrogen (€ m^{-3}), supplier – Air liquide	0.18
EDF electricity tariff (€.MWh^{-1}) in France	60

the regeneration step. The parameters required for the cost analysis were tabulated in Table 6.

4. Results and discussion

4.1. Adsorption step

The breakthrough curve of dichloromethane adsorption on ACM404 was measured during adsorption cycle and it was shown in Fig. 3. Breakthrough curves represent the concentration of VOC (dichloromethane) start to rise in the exit of the column and it was measured by the FID [10]. The amount of dichloromethane adsorbed was calculated by estimating the first momentum of the breakthrough curve. And the adsorption capacity can be calculated by the ratio of the mass of dichloromethane adsorbed to the mass of ACM404 (activated carbon). The adsorption capacity calculated by this method was found to be 31% from the first adsorption cycle. The breakthrough time was determined based on 10% of the concentration of dichloromethane, which is set for adsorption in the inlet stream. The breakthrough time is 188 min as shown in Fig. 3. The dynamic adsorption capacity value (3.7 mol kg^{-1}) was verified if it is close to the value of the equilibrium adsorption capacity value (3.9 mol kg^{-1}). The dynamic adsorption capacity value was calculated by the ratio of dichloromethane in 'moles' to the mass of activated carbon in 'kg' and these values are taken from the dynamic adsorption experiments which generates the breakthrough curves. The equilibrium adsorption capacity was calculated by the ratio of dichloromethane in 'moles' to the mass of activated carbon in 'kg' and these values are taken from the equilibrium adsorption isotherm experiments which are conducted at 20, 40, 60, and 80 °C.

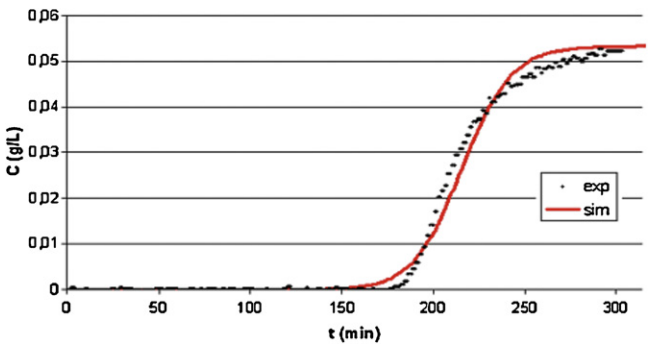

Fig. 3. Experimental and simulation breakthrough curves comparison.

The error deviation between the dynamic and equilibrium adsorption capacity was found to be 5%.

The simulation model PROSIM was executed to compare the results of the experimental and simulated break through curve, temperature profile and it is shown in Figs. 3 and 4. The simulation model results had a good agreement with the experimental results and it has been shown in Figs. 3 and 4.

In Fig. 3, there was a slight deviation between the experimental and the simulation breakthrough curve and it could be explained because of the mass transfer coefficient between the simulation and experimental results. But the discrepancy percentage on the basis of mass of dichloromethane between the experimental and simulation results is less than 2% and it can be neglected. In Fig. 4, there has been also good agreement of temperature profile between the experimental and the simulation results.

4.2. Regeneration step

The operating conditions (temperature of nitrogen, intermediate regeneration, and flow rate of hot nitrogen) of the six regeneration cycles and the corresponding FED responses which are measured as recovery efficiency (F_R) and operating costs ($OP_€$) are presented in Table 7 and Fig. 5. The reason for two sets of 2×2 FEDs instead of just a 3×3 FED is that the flow rate of N_2 at 0.07 L s^{-1} is too low to achieve the superior limit of intermediate regeneration of 75%.

In all the regeneration profiles (Fig. 6), there was a clear shoot after hot nitrogen regeneration where the vacuum regeneration started. This jump occurs from the change in the flow rate of nitrogen (0.018 L s^{-1}) during the vacuum mode. The experimental regenerations and the corresponding simulation runs show that there was discrepancy of 10–12% based on the calculated recovered dichloromethane mass. An example of regeneration temperature profile of the experiment and the simulation was shown in the Fig. 7. From the Table 7 and Fig. 6, it is clear that the recovery efficiency (82%), average regeneration rate (1.74 g min^{-1}) for regeneration 1 was the best operating conditions among the other conditions. The cost was slightly higher than regeneration 3, but it regenerates significantly more than the other experiments. This will also result in retaining good adsorption capacity in the successive adsorption cycle. With these results and the FED factors (in Table 7), it led to form two different 2X2 FED and they are as follows:

1. First set of FED – factors of temperature and intermediate regeneration (Table 7, experiments 1–4)
2. Second set of FED – factors of temperature and flow rate of N_2 (Table 7, experiments 3–6)

4.3. Vacuum cooling effect

Fig. 7 illustrates that the vacuum regeneration (just after hot nitrogen regeneration) decreased the temperature difference of 33 °C in the activated carbon bed. It will enable to save the cost and

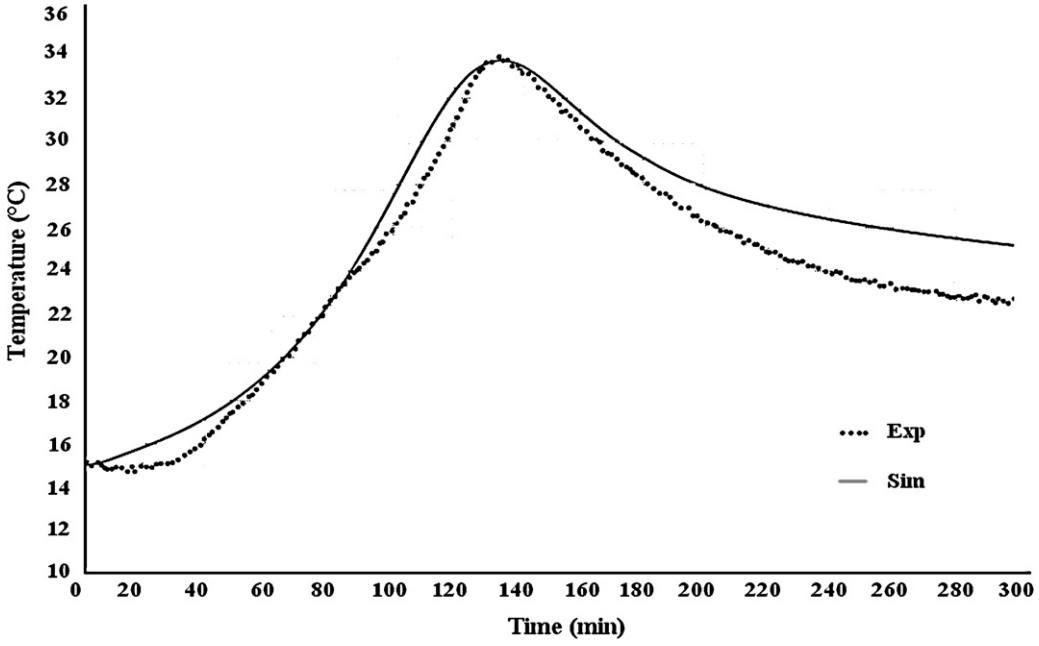

Fig. 4. Experimental and simulation adsorption temperature profile comparison.

Table 7
Recovery efficiency and operating costs results.

Exp.	Operating conditions FED factors			FED responses		Supplementary responses	
	T_{N_2} (°C)	Flow N_2 (N L h^{-1})	I_R (%)	F_R %	$OP_€$ (€ cents)	$OP_€$ (€ kg^{-1})	Recovery (g min^{-1})
1	93	0.14	75	82	64	2.04	1.74
2	85	0.14	75	80	66	2.16	1.70
3	93	0.14	55	74	51	1.80	1.57
4	85	0.14	55	70	53	1.98	1.49
5	93	0.07	55	65	65	2.61	1.13
6	85	0.07	55	62	66	2.78	1.08

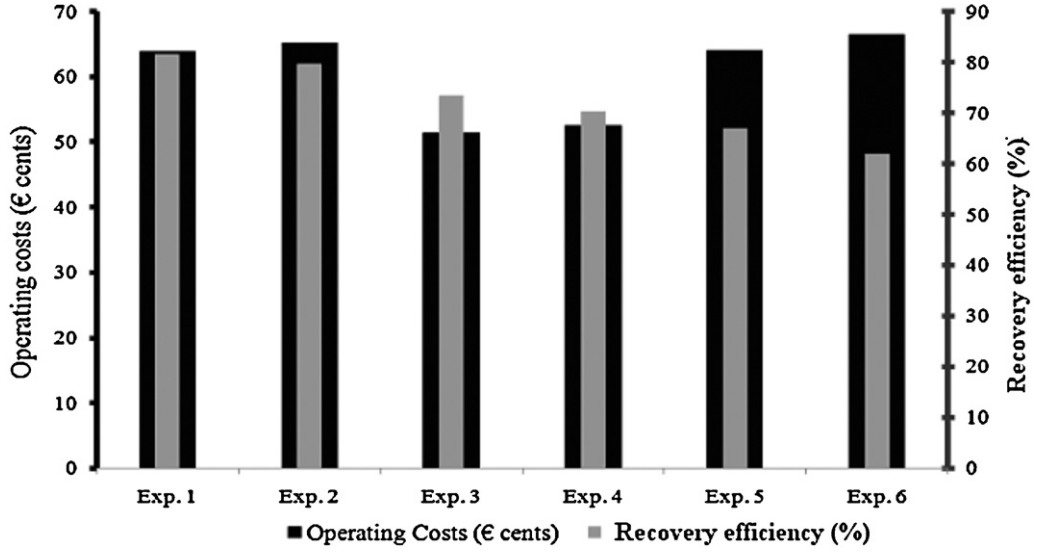

Fig. 5. 0perating costs and recovery efficiency results for regeneration.

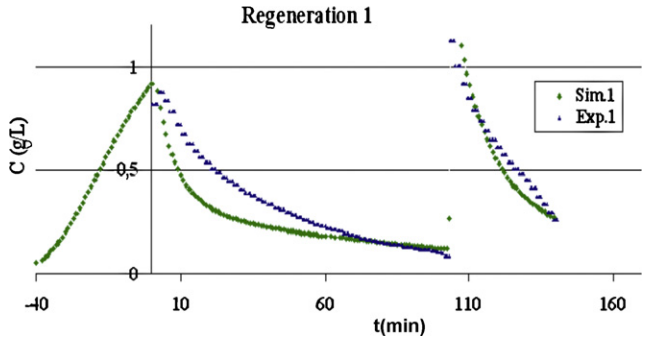

Fig. 6. Regeneration profiles corresponding to operating conditions in Table 7.

reduce the time of the cooling step and thus it proved the advantage of using vacuum regeneration in the combination mode.

4.4. Statistical analysis of regeneration results

The influence of variation of each operating conditions on the recovery efficiency and operating costs were studied by using the FED. The variation of operating conditions such as temperature of nitrogen, intermediate regeneration, and flow rate of nitrogen have their inferior limit (−1) and superior limit (+1). Temperature of nitrogen = ($85_{[-1]}$, $93_{[+1]}$) in °C; intermediate regeneration = ($55_{[-1]}$, $75_{[+1]}$) in %; and flow rate of nitrogen = ($0.07_{[-1]}$, $0.14_{[+1]}$) in L s^{-1}.

With the statistical package MINITAB, it was possible to check the statistical significance of the factors considered in the two sets of FED. The ANOVA were done for the two sets of FED by MINITAB and the solutions are presented as Eqs. (12)–(15). The normalization of the data was done by Fischer's test and the value p (f) is 8%. The effect of operating conditions such as T, I_R and V_f on recovery efficiency and operating costs could be visualized by comparing the significance of the coefficients of T, I_R and V_f from the Eqs. (12)–(15).

It seems that the flow rate dominates the other factors in terms achieving high recovery efficiency and also significantly reducing the operating cost. The factor intermediate regeneration plays a critical role in achieving high recovery efficiency, but it increases the operating costs. The increase in the operating cost was justified by obtaining higher recovery efficiency and so that the number of successive regeneration cycles can be reduced. The interaction effect of temperature and the intermediate regeneration was very low in both cases of recovery efficiency and operating costs and it can be noticed from the value of coefficient of $T{\cdot}I_R$ from Eqs. (12) and (13). From Eqs. (14) and (15), the interaction effects of temperature and flow rate ($T{\cdot}V_f$) were not significant. The first FED set with temperature of nitrogen (T) and intermediate regeneration (I_R) as factors:

$$F_R = 76.5 + 1.5 \cdot T + 4.5 \cdot I_R + 0.5 \cdot T \cdot I_R \quad (12)$$

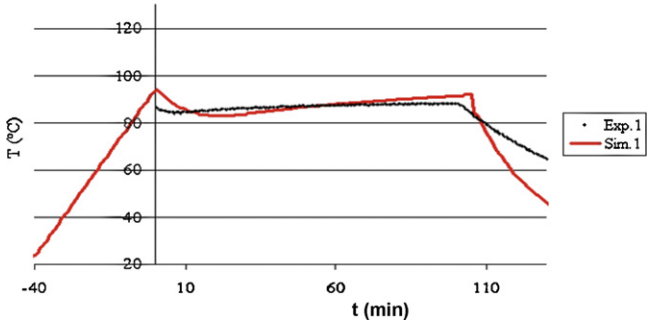

Fig. 7. Regeneration temperature profile at the exit of the column.

$$OP_{€\ cents} = 58.3 - 0.7 \cdot T + 6.3 \cdot I_R + 0.25 \cdot T \cdot I_R \quad (13)$$

where F_R – recovery efficiency and $OP_{€\ cents}$ – operating costs. The second FED set with temperature of nitrogen (T) and flow rate of nitrogen (V_f) as factors

$$F_R = 66.3 + 2.3.T + 5.8 \cdot V_f - 0.25 \cdot T \cdot V_f \quad (14)$$

$$OP_{€\ cents} = 65 - 1 \cdot T - 13 \cdot V_f \quad (15)$$

5. Conclusion

FED was an effective tool to understand how the operating conditions of regeneration influences in the objectives of achieving higher recovery efficiency at an optimized operating cost. The influence of flow rate of hot nitrogen has been significant in increasing the recovery efficiency and decreasing the operating cost. The increase of intermediate regeneration has enabled to achieve maximum recovery efficiency at a shorter total regeneration time. By achieving higher recovery efficiency, it maintains the higher adsorption capacity for the successive cycles of adsorption. The temperature impact was slight (because of slight variation of temperature range) in terms of achieving higher recovery efficiency and optimized operating cost. It could have been interesting, if the heating equipments of higher capacity could have been used, so that the temperature of nitrogen could reach up to 170 °C during thermal regeneration mode. The effect of vacuum regeneration was proven in terms of (1) achieving further effective recovery of dichloromethane after the thermal regeneration mode; (2) cooling of activated carbon bed significantly. It could be more interesting to study the 3 × 3 FED factors effect (temperature of nitrogen, intermediate regeneration and the flow rate of nitrogen) in one design approach of experiments by increasing the capacity of heating equipments.

Acknowledgement

The authors acknowledge the French Environment and Energy Management Agency ADEME, for their excellent scientific collaboration and for funding the research work.

References

[1] EUR-lex, Access to European law. Directive 2004/42/EC of the European Parliament and of the Council. http://eur-lex.europa.eu/en/index.htm, April, 2004 (accessed 19.06.11).
[2] U.S. Environmental Protection Agency, Office of Pollution Prevention and Toxics (OPPT), Dichloromethane Fact Sheet – EPA 749-F-94-018, http://www.epa.gov/chemfact/f_dcm.txt, August, 1994 (accessed 19.06.11).
[3] K.S. Hwang, D.K. Choi, S.Y. Gong, S.Y. Cho, Adsorption and thermal regeneration of methylene chloride vapor on activated carbon bed, Chem. Eng. Process. 46 (1998) 1111–1123.
[4] European Parliament, Health and Environment Dichloromethane to be Banned in Paint-Strippers, REF: 20090113IPR46095, http://www.europarl.europa.eu, January, 2009 (accessed 19.06.11).
[5] P. Pre, F. Delage, P. Le Cloirec, A model to predict the adsorber thermal behavior during treatment ofvolatile organic compounds onto wet activated carbon, Environ. Sci. Technol. 36 (2002) 4681–4688.
[6] F. Delage, P. Pre, P. Le Cloirec, Mass transfert and warming during adsorption of high concentrations of VOCs on an activated carbon bed: experimental and theoretical analysis, Environ. Sci. Technol. 34 (2000) 4816–4821.
[7] P. Pre, F. Delage, P. Le Cloirec, Modeling the exothermal nature of V.O.C. adsorption to prevent activated carbon bed ignition, Fundamen. Adsorption 7 (2001) 1172–1185.
[8] S. Giraudet, H. Tezel, P. Pre, P. Le Cloirec, Estimation of adsorption energies using physical characteristics of activated carbons and VOCs molecular properties, Carbon 44 (2006) 1873–1883.
[9] J. Wu, L.G. Hammarstrom, O. Claesson, I. Fangmark, Modeling the influence of physico-chemical properties of volatile organic compounds on activated carbon adsorption capacity, Carbon 41 (2003) 1322–1325.
[10] EPA Technical Bulletin Report, Choosing an Adsorption System for VOC, Clean Air Technology Centre (CATC), http://www.epa.gov/ttn/catc/dir1/fadsorb.pdf, May, 1999 (accessed 19.06.11).
[11] D.M. Ruthven, Principles of Adsorption and Adsorption Processes, John Wiley & Sons/Univ of New Brunswick, New-York/Fredericton, USA, 1984.

[12] L.K. Wang, N.C. Pereira, Y.T. Hung, Air Pollution Control Engineering, vol. 1, Humana Press, Totowa, NJ, 2004.
[13] R.C. Nattkemper, Nitrogen vs Steam Regeneration in Activated Carbon Systems, American Carbon Society, Imation Corp., Camarillo, CA, 1997, July.
[14] J. Gu, N.M. Faqir, H.J. Bart, Drying of an activated carbon column after steam regeneration, Chem. Eng. Technol. 22 (1999) 859–864.
[15] R.H. Zanitsch, R.T. Lynch, Carbon Adsorption Handbook, Selecting a Thermal Regeneration System for Activated Carbon, Calgon Carbon Corporation, 1997.
[16] T. Boger, A. Salden, G. Eigenberger, A combined vacuum and temperature swing adsorption process for the recovery of amine from foundry air, Chem. Eng. Pro. 36 (1997) 231–242.
[17] P.M. Berthouex, L.C. Brown, Statistics for Environmental Engineers, Lewis Publishers, USA, 2002.
[18] S. Giraudet, P. Pre, P. Le Cloirec, Modeling the heat and mass transfer in temperature swing adsorption of volatile organic compounds on to activated carbons, Environ. Sci. Technol. 43 (2009) 1173–1179.
[19] J. Keller, R. Staudt, Gas Adsorption Equilibria, Universitat Siegen, Springer, USA, 1994.
[20] E.W. Washburn, Note on method of determining the distribution of pore sizes in a porous material, Proc. Natl. Acad. Sci. 7 (1921) 115–116.
[21] T. Jayabalan, Study of Oxidation of Carbon Materials, Ph.D. Dissertation, Ecole des Mines de Nantes, France, 2008.
[22] J.F. Nastaj, B. Ambrożek, J. Rudnicka, Simulation studies of a vacuum and temperature swing adsorption process for the removal of VOC from waste air streams, Int. Commun. Heat Mass Transfer 33 (2006) 80–86.